Int. J. Adv. Appl. Math. and Mech. 4(3) (2017) 60 – 71 (ISSN: 2347-2529)

Journal homepage: www.ijaamm.com

IJAAMM

International Journal of Advances in Applied Mathematics and Mechanics

A multi-regions SEIRS discrete epidemic model with a travel-blocking vicinity optimal control approach on cells

Research Article

Fadwa El Kihal, Mostafa Rachik, Omar Zakary, Ilias Elmouki*

Laboratory of Analysis, Modeling and Simulation (LAMS), Department of Mathematics and Computer Science, Hassan II University of Casablanca. BP 7955, Sidi Othman, Casablanca, Morocco

Received 18 January 2017; accepted (in revised version) 20 February 2017

Abstract: Compared to Susceptible-Infected-Removed Susceptible (SIRS) systems, where it is supposed that a removed population has lost its immunity after being healed from an infection and moves to the susceptible compartment, the S-Exposed-I-R-S (SEIRS) compartmental models, consider also, the presence of an additional compartment named by the variable E which could represent the number of asymptomatic infected individuals, people who are not yet infectious or just exposed to infection. Based on these assumptions, we devise a multi-regions SEIRS discrete-time model which describes infection dynamics due to the presence of an epidemic in regions that are connected with their neighbors by any kind of anthropological movement. The main goal from this kind of modeling, is to introduce after, controls variables which restrict movements of the infected individuals coming from the vicinity of the region targeted by our control strategy we call here by the travel-blocking vicinity optimal control approach. A grid of colored cells is presented to illustrate the whole domain affected by the epidemic while each cell represents a sub-domain or region. In order to illustrate an example of these SEIRS dynamics, we choose an example of infection which is supposed starting from only one cell located in one of the corners of the grid, while the region aiming to control, is supposed to be located in the 2nd line and 4th column of the grid. It is important to note, this optimization approach could be applied to any cell of the grid, and the source of infection could also be supposed to start from any cell. In fact, the example is presented, just to show the effectiveness of the proposed control strategy when it is applied to a cell with an important number of connections (i.e. with 8 neighboring cells in our simulations).

MSC: 93C15 • 34B15

Keywords: Multi-regions model • SEIRS epidemic model • Discrete-time model • Optimal control • Vicinity • Travel-blocking

1. Introduction

Over the last decades, modeling approaches in epidemics have spread the area of epidemiology, and various mathematical models [1],[2] and [3], have been devised for the analysis of the evolution of an epidemic based on population systems. In this paper, we are more interested to investigate the advantages of new modeling and optimal control approaches which aim to describe the impact of movements of infected individuals in different geographical regions, and which could also be applied in the case of regions that are not necessarily attached, but connected by mobility of their people, travel or direct mode of transport, trade activities, etc.

In epidemics, we can sometimes face situations where a removed population has lost its immunity after being healed from an infection, and then, it moves to the susceptible compartment as studied in [4],[5] and [6]. Compartmental models in the form of S-Exposed-I-R-S (SEIRS) models, could well-describe these phenomena. Such systems are very useful to model the evolution of some particular cases, see as example, subject treated in [7].

* Corresponding author.
E-mail address(es): i.elmouki@gmail.com (Ilias Elmouki).

A new modeling approach based on multi-regions discrete-time and continuous-time SIR models, have been proposed by Zakary et al. in [8],[9],[10] and [11], and aimed to describe the spatial-temporal evolution of epidemics which emerge the infe different geographical regions and to show the influence of one region on an other region via infection travel. The authors have also suggested some control strategies such as awareness, vaccination an travel-blocking approaches which could prevent some particular infectious diseases such as HIV/AIDS and Ebola, or epidemics in general, from spreading more.

Here, we suppose the region that we aim to control, to be infected due to movements of infected people which enter only from its neighboring regions, with the hypothesis that in all regions, the removed individuals lose an amount of their immunity.

For this, we suggest here, an other new modeling approach which is based on a multi-regions SEIRS discrete-time epidemic model describing the spatial-temporal spread of an epidemic which emerges in a global domain of interest Ω represented by a grid of colored cells which are uniform in size. These cells are supposed to be connected by movements of their populations, and they represent sub-domains of Ω or regions, noting that only one of these cells, that is targeted by our control strategy.

In [8], each region was represented by a sub-domain $(\Omega_j)_{j=1,..,p}$ while here, each region or cell is denoted by $(C_{pq})_{p,q=1,..,M}$.

For this, we assume that the epidemic can be transmitted and propagated by movements of people, from one spatial cell C_{pq}, to its neighbors or cells belonging to its vicinity. In fact, in a geographical scale relatively small, some infectious diseases such as African Swine Fever [12], Bovine Viral Diarrhoea virus [13],[14] and Foot-and-Mouth Disease [15], follow that pattern of spread, and C_{pq} can represent a farm, while in a large geographical scale such as in the case of Ebola Virus [11], SARS [16], HIV/AIDS [10],[17],[18], and ZIKA Virus [3],[19], a cell C_{pq} can represent a city or country. Thus, the multi-cells model with the vicinity optimal control strategy proposed here, can represent good approaches for infection dynamics studies regardless of the area size. In fact, the optimization criteria are chosen here in a way to restrict movements of people coming from one or more cells and entering other cells. Explicitly, we seek to minimize an objective function associated to C_{pq}, subject to its associated discrete-time system, with optimal control functions introduced into the SEIRS systems, to show the effectiveness rates of the travel-blocking operations followed between C_{pq} and its neighbors. We note by V_{pq}, the vicinity set, composed by all neighboring cells of C_{pq} and which are denoted by $(C_{rs})_{r=p+k,s=q+k'}$ with $(k,k') \in \{-1,0,1\}^2$ except when $k=k'=0$. Note also as we have mentioned before, these cells are attached just in the grid, but in reality, they are not necessarily joined together. Thus, the travel-blocking vicinity optimal control approach will show the impact of the optimal blocker controls on reducing contacts between susceptible people of the targeted cell C_{pq} and infected people coming from one cell C_{rs} or more cells from V_{pq}.

The paper is organized as follows: Section 2. presents the multi-regions or multi-cells SEIRS epidemic discrete-time systems, based on a colored cell simulation approach. In Section 3., we announce a theorem of necessary conditions and characterization of the sought optimal controls functions related to the travel-blocking vicinity optimal control approach. Finally, in section 4., we provide simulations of the numerical results for an example of 100 cells when an infection starts from one cell of them and which has 3 neighboring cells since it is located in one of the corners of the grid, while aiming to control only one cell with 8 neighboring cells.

2. The mathematical SEIRS model

Explicitly, we consider a multi-regions discrete-time epidemic model which describes SEIRS dynamics within a global domain of interest Ω which in turn is divided to M^2 regions or cells, uniform in size. In other words, $\Omega = \bigcup_{p,q=1}^{M} C_{pq}$ with C_{pq} denoting a spatial location or region.

We note that $(C_{pq})_{p,q=1,...,M}$ could represent a country, a city or town, or a small domain such as neighborhoods, that belong respectively to the global domain of interest Ω which could in turn represent a part of continent or even a whole continent, a part of country or a whole country, etc.

The S-E-I-R populations associated to a cell C_{pq} are noted by the states $S_i^{C_{pq}}$, $E_i^{C_{pq}}$, $I_i^{C_{pq}}$, and $R_i^{C_{pq}}$, and we note that the transition between them, is probabilistic, with probabilities being determined by the observed characteristics of specific diseases. In addition to the death, there are population movements among these three epidemiological compartments, from time unit i to time $i+1$. We assume that the susceptible individuals, are not yet infected but can be infected only through contacts with infected people from V_{pq} (Vicinity set or Neighborhood of a cell C_{pq}), thus, the infection transmission is assumed to occur between individuals present in a given cell C_{pq}, and its incidence rate is given by

$$\sum_{C_{rs} \in V_{pq}} \beta_{rs} I_i^{C_{rs}} S_i^{C_{pq}}$$

where β_{rs} is the constant proportion of adequate contacts between a susceptible from a cell C_{pq} and an infective coming from its neighbor cell $C_{rs} \in V_{pq}$ with

V_{pq}=$\{C_{rs} \in \Omega / r = p+k, s = q+k', (k,k') \in \{-1,0,1\}^2\} \setminus C_{pq}$.
SEIRS dynamics associated to domain or cell C_{pq} are described based on the following multi-cells discrete model
For $p, q = 1, \ldots, M$, we have

$$S_{i+1}^{C_{pq}} = S_i^{C_{pq}} - \beta_{pq} I_i^{C_{pq}} S_i^{C_{pq}} - \sum_{C_{rs} \in V_{pq}} \beta_{rs} I_i^{C_{rs}} S_i^{C_{pq}} - d S_i^{C_{pq}} + \theta R_i^{C_{pq}} \tag{1}$$

$$E_{i+1}^{C_{pq}} = E_i^{C_{pq}} + \beta_{pq} I_i^{C_{pq}} S_i^{C_{pq}} + \sum_{C_{rs} \in V_{pq}} \beta_{rs} I_i^{C_{rs}} S_i^{C_{pq}} - (\gamma + d) E_i^{C_{pq}} \tag{2}$$

$$I_{i+1}^{C_{pq}} = I_i^{C_{pq}} + \gamma E_i^{C_{pq}} - (\alpha + d + \delta) I_i^{C_{pq}} \tag{3}$$

$$R_{i+1}^{C_{pq}} = R_i^{C_{pq}} + \delta I_i^{C_{pq}} - (d + \theta) R_i^{C_{pq}} \tag{4}$$

$i = 0, ..., N-1$
with $S_0^{C_{pq}} \geqslant 0, E_0^{C_{pq}} \geqslant 0, I_0^{C_{pq}} \geqslant 0$ and $R_0^{C_{pq}} \geqslant 0$ are the given initial conditions.

$d > 0$ is the natural death rate while $\alpha > 0$ is the death rate due to the infection, $\gamma > 0$ denotes the average incubation period, $\delta > 0$ is the natural recovery rate from infection, and $\theta > 0$ denotes the immunity loss rate. By assuming that all regions are occupied by homogeneous populations, $d, \alpha, \gamma, \delta$ and θ, are considered to be the same for all cells of Ω.

3. The travel-blocking vicinity optimal control approach

The travel-blocking vicinity optimal control strategy, aims to restrict movements of infected people coming from the vicinity set V_{pq} and intending to reach the cell C_{pq}. For this, we introduce controls $u^{pqC_{rs}}$ variables into the model (1)-(4), to show the effectiveness rate of the travel-blocking approach which limits contacts between susceptible people of the targeted cell C_{pq} and infected individuals of cells C_{rs}. Then, for a given cell C_{pq} in Ω, the discrete-time system (1)-(4) becomes

$$S_{i+1}^{C_{pq}} = S_i^{C_{pq}} - \beta_{pq} I_i^{C_{pq}} S_i^{C_{pq}} - \sum_{C_{rs} \in V_{pq}} u_i^{pqC_{rs}} \beta_{rs} I_i^{C_{rs}} S_i^{C_{pq}} - d S_i^{C_{pq}} + \theta R_i^{C_{pq}} \tag{5}$$

$$E_{i+1}^{C_{pq}} = E_i^{C_{pq}} + \beta_{pq} I_i^{C_{pq}} S_i^{C_{pq}} + \sum_{C_{rs} \in V_{pq}} u_i^{pqC_{rs}} \beta_{rs} I_i^{C_{rs}} S_i^{C_{pq}} - (\gamma + d) E_i^{C_{pq}} \tag{6}$$

$$I_{i+1}^{C_{pq}} = I_i^{C_{pq}} + \gamma E_i^{C_{pq}} - (\alpha + d + \delta) I_i^{C_{pq}} \tag{7}$$

$$R_{i+1}^{C_{pq}} = R_i^{C_{pq}} + \delta I_i^{C_{pq}} - (d + \theta) R_i^{C_{pq}} \tag{8}$$

$i = 0, ..., N-1$
Based on the model with control (5)-(8), we aim to minimize the number of the infected people and the cost of the vicinity optimal control approach. Thus, we consider an optimization criterion associated to cell C_{pq} and we define it by the following objective function

$$J_{pq}(u^{pq}) = A_1 I_N^{C_{pq}} + \sum_{i=0}^{N-1} \left(A_1 I_i^{C_{pq}} + \sum_{C_{rs} \in V_{pq}} \frac{A_{rs}}{2} (u_i^{pqC_{rs}})^2 \right) \tag{9}$$

where $A_1 > 0$ and $A_{rs} > 0$ are the constant severity weights associated to the number of infected individuals and controls respectively. The controls functions are defined in the control set U_{pq} associated to the cell C_{pq}, defined by

$$U_{pq} = \{u^{pqC_{rs}} \ \ measurable / u^{min} \leq u_i^{pqC_{rs}} \leq u^{max}, \ u^{max} < 1 \ u^{min} > 0, \quad i = 0, ..., N-1, C_{rs} \in V_{pq}\} \tag{10}$$

Then, we seek optimal controls $u^{pqC_{rs}*}$ such that

$$J_{pq}(u^{pqC_{rs}*}) = min\{J_j(u^{pqC_{rs}}) / u^{pqC_{rs}} \in U_{pq}\}$$

The sufficient conditions for the existence of optimal controls in this case, are the same as the ones, announced in the case of discrete-time epidemic models [8],[9],[20] and [21].

As regards to the necessary conditions and the characterization of our discrete optimal control, we use a discrete version of Pontryagin's maximum principle [8],[9],[22].

For this, we define a Hamiltonian $\mathscr{H}$ associated to a cell C_{pq} by

$$\begin{aligned}
\mathscr{H} = {} & A_1 I_i^{C_{pq}} + \sum_{C_{rs} \in V_{pq}} \frac{A_{rs}}{2} (u_i^{pqC_{rs}})^2 + \zeta_{1,i+1}^{C_{pq}} \Big[S_i^{C_{pq}} - \beta_{pq} I_i^{C_{pq}} S_i^{C_{pq}} \\
& - \sum_{C_{rs} \in V_{pq}} u_i^{pqC_{rs}} \beta_{rs} I_i^{C_{rs}} S_i^{C_{pq}} - d S_i^{C_{pq}} + \theta R_i^{C_{pq}} \Big] \\
& + \zeta_{2,i+1}^{C_{pq}} \Big[E_i^{C_{pq}} + \beta_{pq} I_i^{C_{pq}} S_i^{C_{pq}} + \sum_{C_{rs} \in V_{pq}} u_i^{pqC_{rs}} \beta_{rs} I_i^{C_{rs}} S_i^{C_{pq}} - (\gamma + d) E_i^{C_{pq}} \Big] \\
& + \zeta_{3,i+1}^{C_{pq}} \Big[I_i^{C_{pq}} + \gamma E_i^{C_{pq}} - (\alpha + d + \delta) I_i^{C_{pq}} \Big] \zeta_{4,i+1}^{C_{pq}} \Big[R_i^{C_{pq}} + \delta I_i^{C_{pq}} - (d + \theta) R_i^{C_{pq}} \Big]
\end{aligned}$$

$i = 0, ..., N-1$
with $\zeta_{k,i}^{C_{pq}}$, $k = 1,2,3,4$, the adjoint variables associated to $S_i^{C_{pq}}$, $E_i^{C_{pq}}$, $I_i^{C_{pq}}$ and $R_i^{C_{pq}}$ respectively, and defined based on formulations of the following theorem.

Theorem 3.1 (Necessary Conditions and Characterization).
Given optimal controls $u^{pqC_{rs}*}$ and solutions $S^{C^*_{pq}}, I^{C^*_{pq}}$ and $R^{C^*_{pq}}$, there exists $\zeta_{k,i}^{C_{pq}}$, $i = 0...N$, $k = 1,2,3,4$, the adjoint variables satisfying the following equations

$$\triangle\zeta_{1,i}^{C_{pq}} = -\left[(1-d)\zeta_{1,i+1}^{C_{pq}} + \left(\beta_{pq} I_i^{C_{pq}} + \sum_{C_{rs}\in V_{pq}} u_i^{C_{rs}} \beta_{rs} I_i^{C_{rs}}\right)\left(\zeta_{2,i+1}^{C_{pq}} - \zeta_{1,i+1}^{C_{pq}}\right)\right] \tag{11}$$

$$\triangle\zeta_{2,i}^{C_{pq}} = -\left[\gamma\left(\zeta_{3,i+1}^{C_{pq}} - \zeta_{2,i+1}^{C_{pq}}\right) + (1-d)\zeta_{2,i+1}^{C_{pq}}\right] \tag{12}$$

$$\triangle\zeta_{3,i}^{C_{pq}} = -\left[A_1 + \beta_{pq} S_i^{C_{pq}}\left(\zeta_{2,i+1}^{C_{pq}} - \zeta_{1,i+1}^{C_{pq}}\right) + (1-\alpha-d)\zeta_{3,i+1}^{C_{pq}} + \delta\left(\zeta_{4,i+1}^{C_{pq}} - \zeta_{3,i+1}^{C_{pq}}\right)\right] \tag{13}$$

$$\triangle\zeta_{4,i}^{C_{pq}} = -\left[\theta\left(\zeta_{1,i+1}^{C_{pq}} - \zeta_{4,i+1}^{C_{pq}}\right) + (1-d)\zeta_{4,i+1}^{C_{pq}}\right] \tag{14}$$

with $\zeta_{1,N}^{C_{pq}} = 0, \zeta_{2,N}^{C_{pq}} = 0, \zeta_{3,N}^{C_{pq}} = A_1, \zeta_{4,N}^{C_{pq}} = 0$, are the transversality conditions.
In addition

$$u_i^{pqC^*_{rs}} = \min\left\{\max\left\{u^{\min}, \frac{(\zeta_{1,i+1}^{C_{pq}} - \zeta_{2,i+1}^{C_{pq}})\beta_{rs} I_i^{C^*_{rs}} S_i^{C^*_{pq}}}{A_{rs}}\right\}, u^{\max}\right\}, \quad i = 0, ..., N-1 \tag{15}$$

Proof. Using a discrete version of Pontryagin's Maximum Principle in [8],[9],[22], and setting $S^{C_{pq}} = S^{C_{pq}*}$, $E^{C_{pq}} = E^{C_{pq}*}$, $I^{C_{pq}} = I^{C_{pq}*}$, $R^{C_{pq}} = R^{C_{pq}*}$ and $u^{pqC_{rs}} = u^{pqC_{rs}*}$ we obtain the following adjoint equations

$$\begin{aligned}
\triangle\zeta_{1,i}^{C_{pq}} &= -\frac{\partial\mathcal{H}}{\partial S_i^{C_{pq}}} \\
&= \left[(1-d)\zeta_{1,i+1}^{C_{pq}} + \left(\beta_{pq} I_i^{C_{pq}} + \sum_{C_{rs}\in V_{pq}} u_i^{C_{rs}} \beta_{rs} I_i^{C_{rs}}\right)\left(\zeta_{2,i+1}^{C_{pq}} - \zeta_{1,i+1}^{C_{pq}}\right)\right] \\
\triangle\zeta_{2,i}^{C_{pq}} &= -\frac{\partial\mathcal{H}}{\partial E_i^{C_{pq}}} \\
&= -\left[\gamma\left(\zeta_{3,i+1}^{C_{pq}} - \zeta_{2,i+1}^{C_{pq}}\right) + (1-d)\zeta_{2,i+1}^{C_{pq}}\right] \\
\triangle\zeta_{3,i}^{C_{pq}} &= -\frac{\partial\mathcal{H}}{\partial I_i^{C_{pq}}} \\
&= -\left[A_1 + \beta_{pq} S_i^{C_{pq}}\left(\zeta_{2,i+1}^{C_{pq}} - \zeta_{1,i+1}^{C_{pq}}\right) + (1-\alpha-d)\zeta_{3,i+1}^{C_{pq}} + \delta\left(\zeta_{4,i+1}^{C_{pq}} - \zeta_{3,i+1}^{C_{pq}}\right)\right] \\
\triangle\zeta_{4,i}^{C_{pq}} &= -\frac{\partial\mathcal{H}}{\partial R_i^{C_{pq}}} \\
&= -\left[\theta\left(\zeta_{1,i+1}^{C_{pq}} - \zeta_{4,i+1}^{C_{pq}}\right) + (1-d)\zeta_{4,i+1}^{C_{pq}}\right]
\end{aligned}$$

with $\zeta_{1,N}^{C_{pq}} = 0, \zeta_{2,N}^{C_{pq}} = 0, \zeta_{3,N}^{C_{pq}} = A_1, \zeta_{4,N}^{C_{pq}} = 0$; the transversality conditions.

In order to obtain the optimality condition, we calculate the derivative of H with respect to $u_i^{pqC_{rs}}$, and we set it equal to zero

$$\frac{\partial\mathcal{H}}{\partial u_i^{pqC_{rs}}} = A_{rs} u_i^{pqC_{rs}} - \zeta_{1,i+1}^{C_{pq}} \beta_{rs} I_i^{C_{rs}} S_i^{C_{pq}} + \zeta_{2,i+1}^{C_{pq}} \beta_{rs} I_i^{C_{rs}} S_i^{C_{pq}} = 0$$

Then, we obtain

$$u_i^{pqC_{rs}} = \frac{(\zeta_{1,i+1}^{C_{pq}} - \zeta_{2,i+1}^{Cpq})\beta_{rs} I_i^{C_{rs}} S_i^{C_{pq}}}{A_{rs}}$$

By the bounds in U_{pq}, we finally obtain the characterization of the optimal controls $u_i^{pqC^*_{rs}}$ as

$$u_i^{pqC^*_{rs}} = \min\left\{\max\left\{u^{\min}, \frac{(\zeta_{1,i+1}^{C_{pq}} - \zeta_{2,i+1}^{C_{pq}})\beta_{rs} I_i^{C^*_{rs}} S_i^{C^*_{pq}}}{A_{rs}}\right\}, u^{\max}\right\}, \quad i = 0, ..., N-1, , C_{rs} \in V_{pq} \tag{16}$$

□

Table 1. Parameters values of α, β, γ, d, δ and θ associated to a cell C_{pq}, $p,q = 1,...,M$, and which are utilized for the resolution of all multi-regions discrete-time systems (1)-(4) and (5)-(8), and then leading to simulations obtained from Fig. 1 to Fig. 6, with the initial conditions $S_0^{C_{pq}}, E_0^{C_{pq}}, I_0^{C_{pq}}$ and $R_0^{C_{pq}}$ associated to any cell C_{pq} of Ω.

$S_0^{C_{pq}}$	$E_0^{C_{pq}}$	$I_0^{C_{pq}}$	$R_0^{C_{pq}}$	α	β	γ	d	δ	θ
50	0	0	0	0.002	0.0001	0.002	0.0001	0.003	0.0002

4. Numerical results and discussions

4.1. Brief presentation

We present now, the obtained numerical simulations in the case when the studied domain Ω represents the assembly of M^2 regions or cells (cities, towns, ...). We write and compile a code in MATLAB using data from Table 1. The multi-points boundary value problems are solved using an iterative method where at instant i, the states $S_i^{C_{pq}}$, $E_i^{C_{pq}}$, $I_i^{C_{pq}}$, and $R_i^{C_{pq}}$ with an initial guess, are obtained based on a progressive scheme in time, and their adjoint variables $\zeta_{l,i}^{C_{pq}}, l = 1,2,3,4$ are obtained based on a regressive scheme in time because of the transversality conditions. Then, we update the optimal controls values (15) using the values of state and costate variables obtained in the previous steps. Finally, the previous steps are executed until we reach a tolerance criterion. In order to show the importance of our work, and without loss of generality, we consider here that $M = 10$, and then, we present our results in a 10×10 grid.

Note that, at $i = 0$, the susceptible people are homogeneously distributed with 50 individuals in each cell except at the upper-right corner cell C_{110} where we introduce 10 infected individuals and 40 susceptible ones.

In all of the figures below, the redder part of the color-bars, contains larger numbers of individuals while the bluer part contains the smaller numbers.

In the following, we discuss with more details, the cellular simulations we obtain, in the case when there are yet no controls.

4.2. Cellular simulations without controls

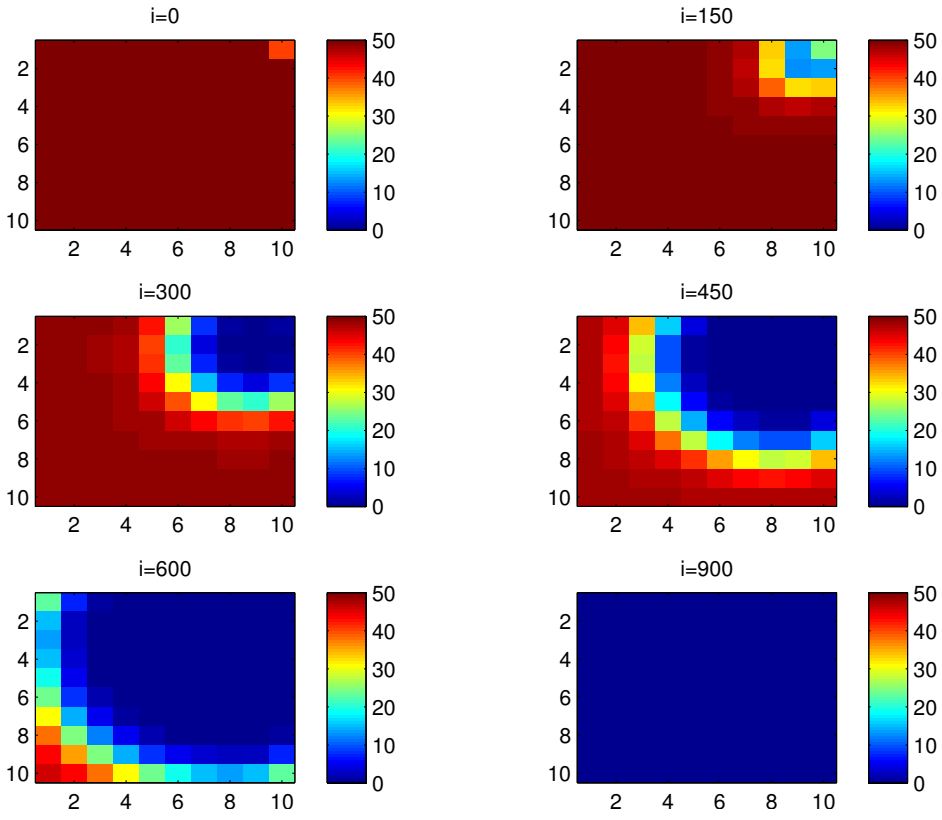

Fig. 1. $S^{C_{pq}}$ behavior in the absence of controls.

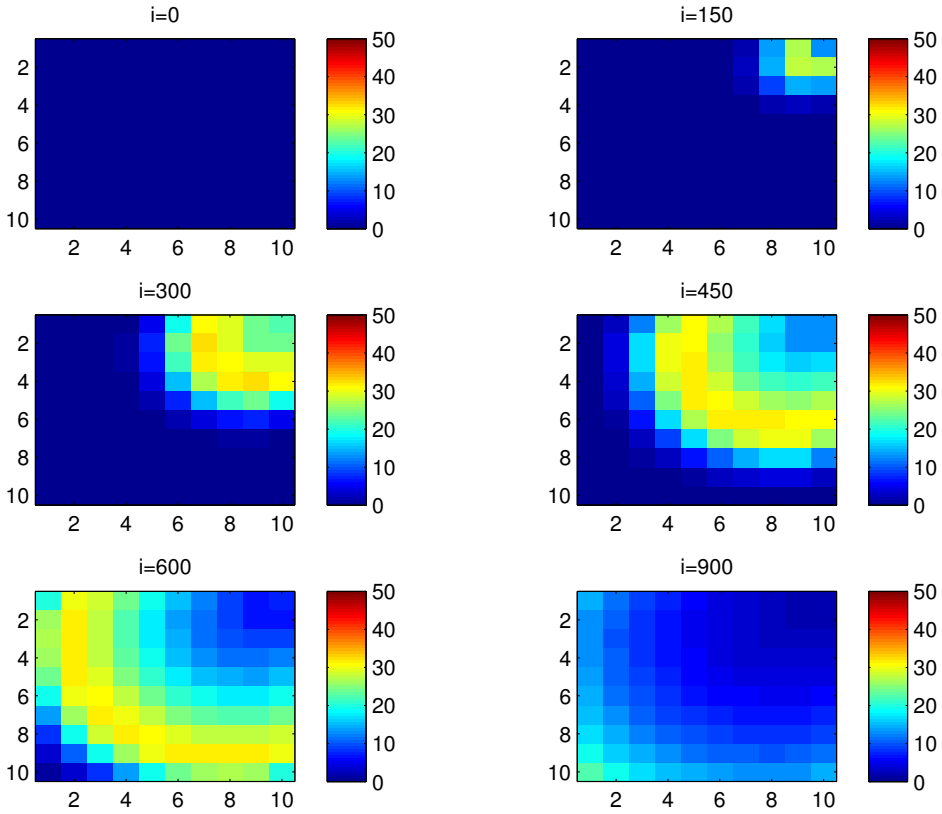

Fig. 2. E^{Cpq} behavior in the absence of controls.

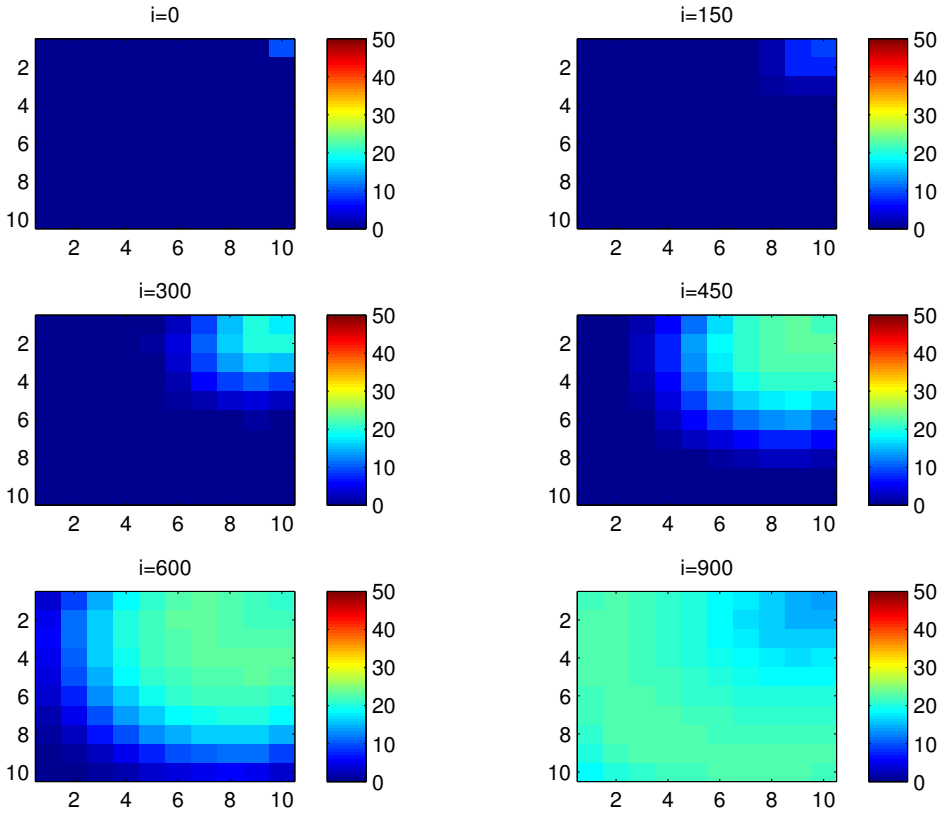

Fig. 3. I^{Cpq} behavior in the absence of controls.

In this section, Figs. 1, 2, 3 and 4 depict dynamics of the susceptible, exposed, infected and removed populations in

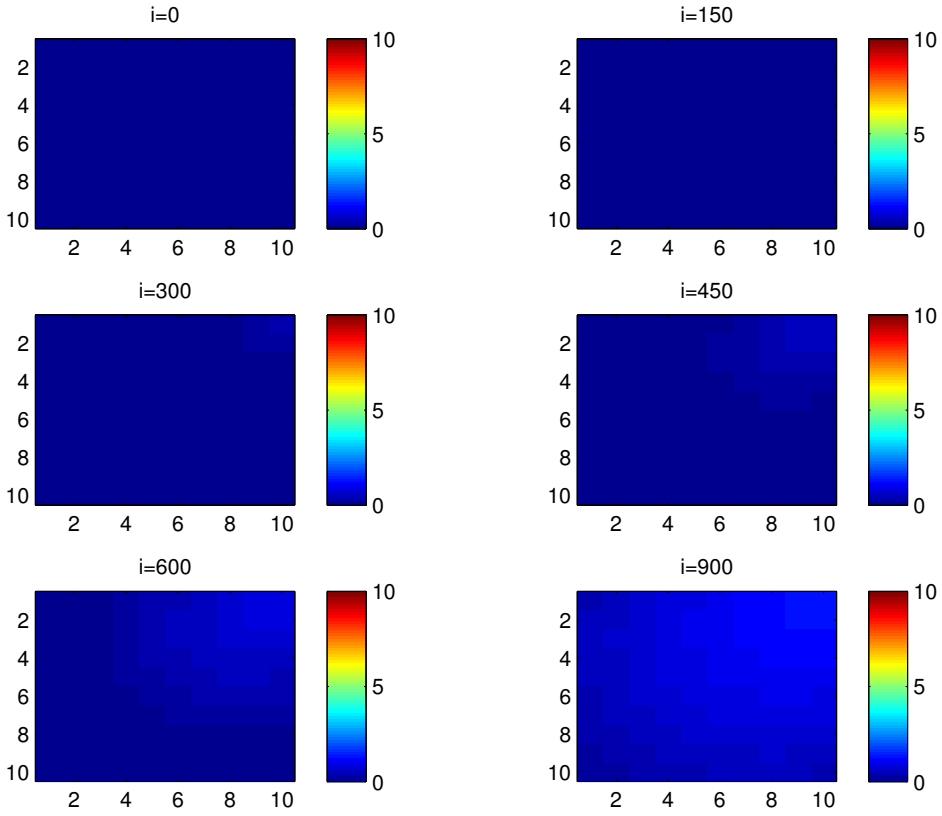

Fig. 4. $R^{C_{pq}}$ behavior in the absence of controls. The color-bars scales here, are fixed to 10 as maximal values, because of small obtained values which can not be seen clearly in case of larger color values intervals or which could be confused with the number 10 if we take 50 as maximal number of people.

the case when there is yet no control strategy, followed for the prevention of the epidemic, and we note that in all these figures presented here, simulations give us an idea about the spread of the epidemic in the case when the infection starts in a cell C_{pq} with $p = 1, q = 10$ (located in the upper-right corner of Ω). In fact, this represents the case when the vicinity set V_{pq} associated to the source cell of infection, contains 3 cells).

For instance, in Fig. 1, if we suppose there are 40 susceptible people in cell C_{110} located at the upper-right corner of Ω, and 50 in each other cell, we can see that at instant $i = 150$, the number $S^{C_{110}}$ becomes less important and takes a value close/or equal to 20, while $S^{C_{pq}}$ in cells of V_{110} take values close/or equal to 30, and as we move away from $V_{110} = \{C_{19}, C_{29}, C_{210}\}$, $S^{C_{pq}}$ remains important. At instant $i = 300$, we can observe that in most cells, $S^{C_{pq}}$ becomes less important, taking values between 0 and 10 in cells which are close to the source of infection, while in other cells, it takes values between 20 and 40 except $S^{C_{101}}$ and in the neighboring cells of C_{101}, they conserve their values in 50 since it is located far away from the source of infection. At instant $i = 450$, $S^{C_{pq}}$ becomes zero except at the opposite corners and in most cells at the borders of Ω because these cells have vicinity sets smaller than other cells. Finally at last instants, $S^{C_{pq}}$ converge to zero in all cells.

Fig. 2 the infection when the disease starts from cell C_{110}. In Fact, if we suppose there are 10 infected people in cell C_{110}, and no infection in all other cells, we observe that at instant $i = 150$, the number $E^{C_{110}}$ increases to bigger values close/or equal to 30 in C_{29}, while $E^{C_{pq}}$ in other cells of V_{110} takes values close/or equal to 25, and as we move away from V_{110}, $E^{C_{pq}}$ remains less important. At instant $i = 300$, we can see that in most cells, $E^{C_{pq}}$ becomes more important, taking values between 30 and 35 in cells which are close to V_{110} and in cells with 8 neighboring cells, while in the other cells, it takes values between 0 and 20. From these numerical results, we can deduce that once the infection arrives to the center or to the cells with 8 cells in their vicinity sets, the exposure to infection becomes more important compared to the case of the previous instant. At instant $i = 450$, $E^{C_{pq}}$ takes values close/or equal to 15 in the cell from where the epidemic has started, and 25 in cells which are close to V_{110}, and as we move away towards the center and further regions, exposure to infection is important with the presence of more than 30 exposed individuals in some cells except the ones which are more close to the 3 opposite corners even at instant $i = 600$. In fact, at the center of Ω, the number of exposed people which has increased to 35 at the previous instant, has been reduced, because once a cell becomes highly infected, it loses an important number of individuals which die or recover naturally after. All cells C_{pq} become highly exposed and the number $E^{C_{pq}}$ becomes less and less important at further instants, noting that at $i = 900$, a large number of exposed individuals, has decreased because many $E^{C_{pq}}$ have died or moved to the infected compartment.

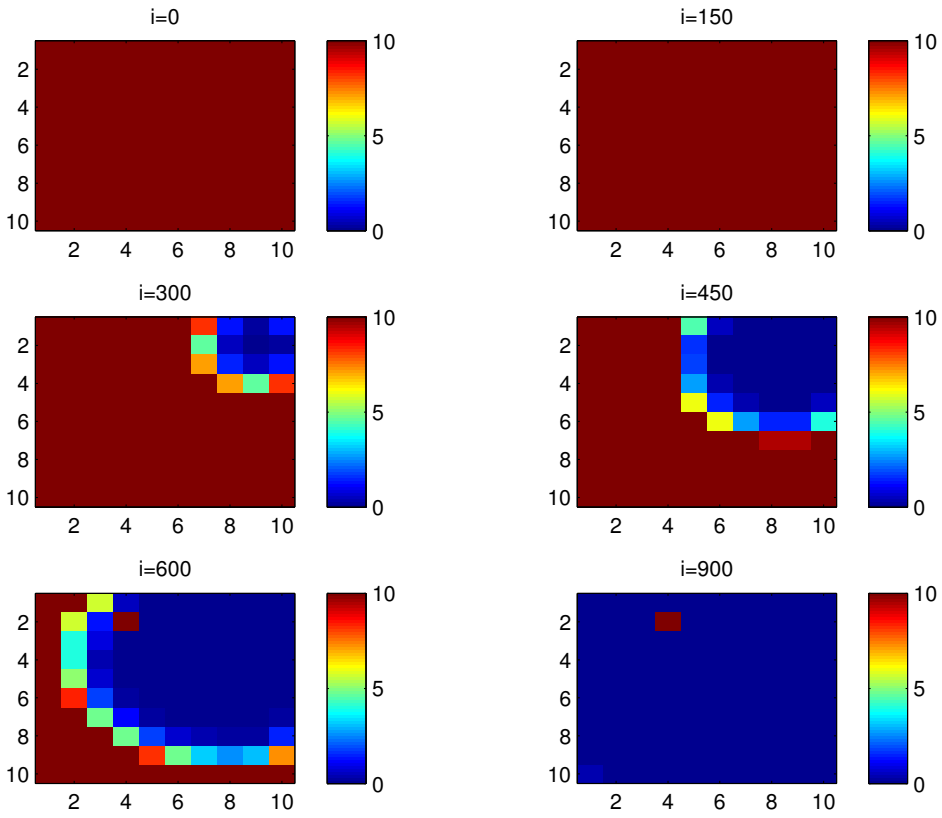

Fig. 5. $S^{C_{pq}}$ behavior in the presence of optimal controls (15). The color-bars scales here, are fixed to 10 as maximal values, because of small obtained values which can not be seen clearly in case of larger color values intervals or which could be confused with the number 10 if we take 50 as maximal number of people.

In Fig. 3, we can observe more the spatial spread of infection in regions or cells of Ω, when we consider a nonzero initial condition of infection in the upper-right corner cell C_{110} only. In fact, at instant $i = 150$, the number $I^{C_{110}}$ and $I^{C_{pq}}$ in cells of V_{110} are close/or equal to only 10 or less, and as we move away from V_{110} more and more, $I^{C_{pq}}$ becomes zero. Similarly, at instant $i = 300$, the number $I^{C_{pq}}$ is not zero and takes values between 1 and 3, except for distant cells where it remains zero. At instant $i = 450$, $I^{C_{pq}}$ takes values between 10 and 15 except at the opposite 3 corners to infection, and some cells at the borders where there are yet no infected people. Finally, at further instants $I^{C_{pq}}$ converge to 20 in most cells at $i = 600$, and in all cells at $i = 900$, since as more we go forward in time, some people acquire immune responses that help them to cure naturally from the disease.

As we can observe in Fig. 4, when we have supposed there are 40 susceptible people in cell C_{110}, and 50 in each other cell, we can see here that simultaneously, at instant $i = 150$, the number $R^{C_{110}}$ and $R^{C_{pq}}$ in cells of V_{110} are close/or equal to only 1 or two removed people, and as we move away from V_{110}, $R^{C_{pq}}$ remains zero. Similarly, at instant $i = 300$, the number $R^{C_{pq}}$ is not zero and takes values between 1 and 3, except for distant cells where it remains zero. At instant $i = 450$, $R^{C_{pq}}$ takes values between 3 and 5 except at the opposite 3 corners and some cells at the borders where it does not exceed 2 removed people. Finally, at further instants $R^{C_{pq}}$ converge to 5 in most cells at $i = 600$ and in all cells at $i = 900$ since as more we go forward in time, some people acquire immune responses that help them to cure naturally from the disease.

4.3. Cellular simulations with controls

Figs. 5, 6, 7 and 8 depict dynamics of the SEIRS populations when the travel-blocking vicinity optimal control strategy is followed.

In order to show the importance of the optimal control approach suggested in this paper, we take the example of a cell which has 8 neighboring cells, and as done in the previous part, we investigate also here, the results obtained when the disease starts from cell C_{110} located in the upper border of Ω. As an example, we suppose that the cell we aim to control is C_{24}.

In Fig. 5, as supposed also above, there are 40 susceptible people in cell C_{110}, and 50 in each other cell. We can see that at instant $i = 150$, the numbers $S^{C_{110}}$ and $S^{C_{pq}}$ are at most the same as in the case when there was no control strategy, because of the small color-bars scale which hides the values of $S^{C_{pq}}$ that are in/or near the source of infection. In fact, because of small values which do not exceed 10 individuals when going forward in time, the scale has

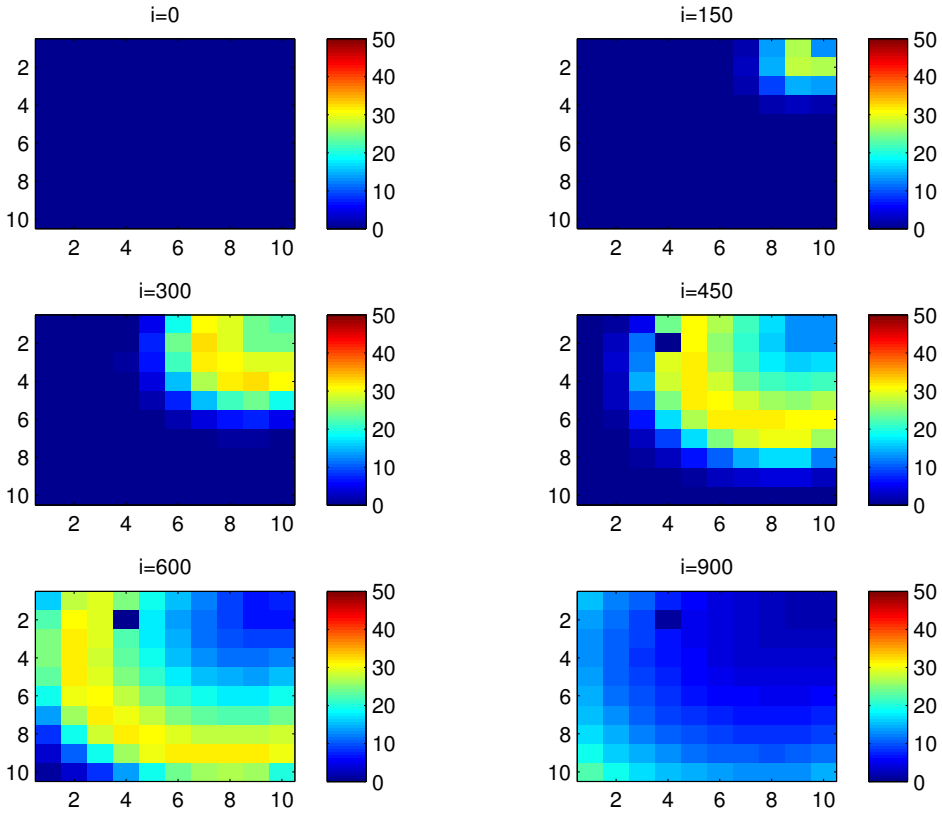

Fig. 6. $E^{C_{pq}}$ behavior in the presence of optimal controls (15).

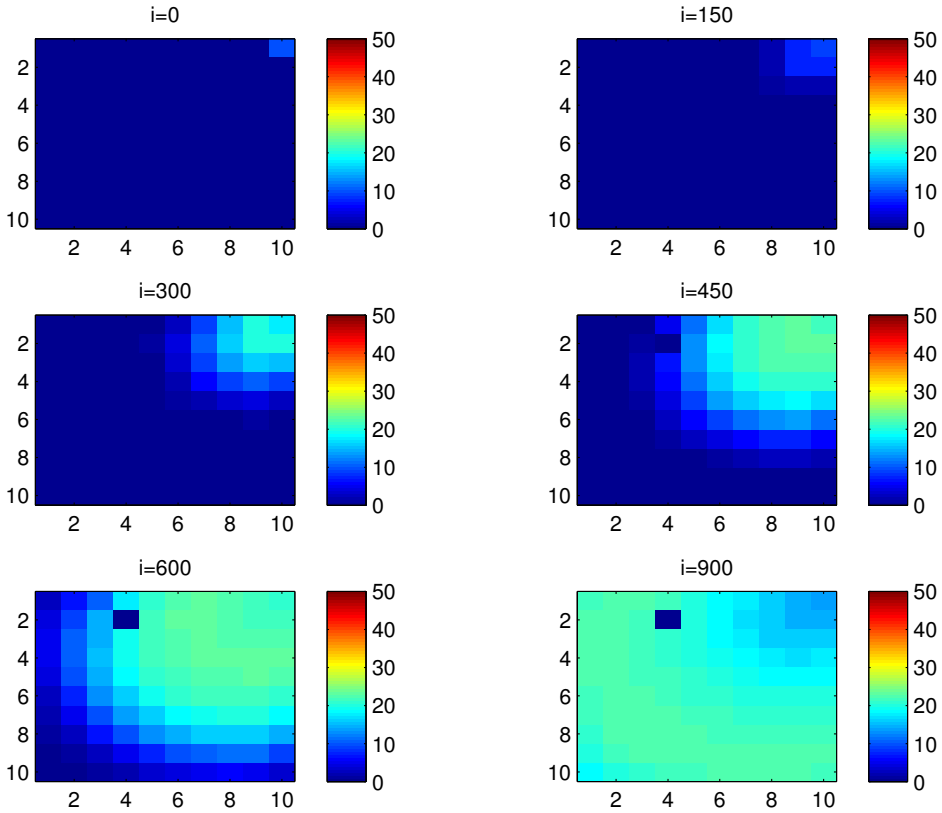

Fig. 7. $I^{C_{pq}}$ behavior in the presence of optimal controls (15).

been fixed in 10 from $i = 0$ until final times, to see the evolution of the epidemic with same values intervals to avoid

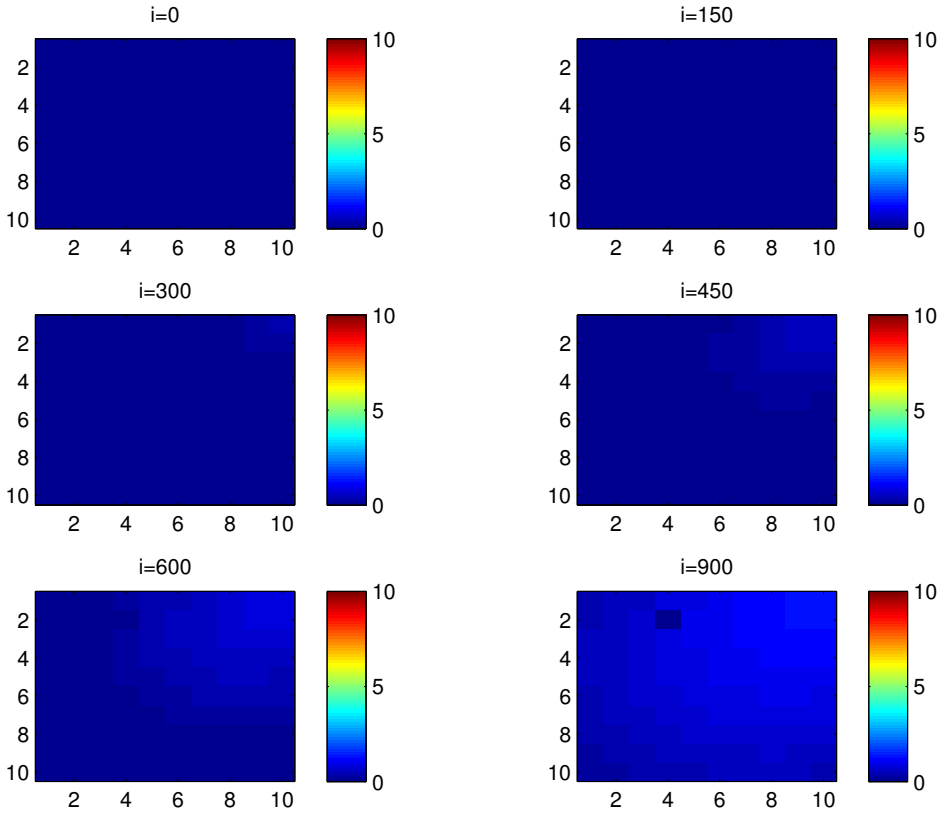

Fig. 8. $R^{C_{pq}}$ behavior in the absence of controls. The color-bars scales here, are fixed to 10 as maximal values, because of small obtained values which can not be seen clearly in case of larger color values intervals.

confusion. At instant $i = 300$, we can observe that $S^{C_{pq}}$ becomes less important, taking values between 0 and 10 in cells that are close to V_{110}, while in other cells, and as more we move away from V_{110}, it takes values between 7.5 or more. At instants $i = 450, 600$ and $i = 900$, $S^{C_{pq}}$ takes smaller values but we reach our goal in keeping the number $S^{C_{24}}$ close to its initial value. Thus, this demonstrates that most of movements of infected people coming from the vicinity set $V^{C_{24}}$, have been restricted in final times.

In Fig. 6, when the disease starts from cell C_{110}, as supposed in the section above, there are 10 infected people in cell C_{110}, and no infected in each other cell, and we can deduce that at instant $i = 150$, the numbers $E^{C_{110}}$ and $E^{C_{pq}}$ are at most the same, as shown in the absence of controls. At instant $i = 300$, we can see that in most cells, $E^{C_{pq}}$ is similar to the case presented in Fig. 3, taking values between 20 and 30 while in other cells, it takes values between 0 and 10 as shown in the previous subsection. However, the controlled cell C_{24} is still not really infected and contains only about one infected individual. At instant $i = 450$, $E^{C_{pq}}$ takes values around 20 in neighboring cells which belong to V_{110}, and about 30 in other cells except at the 3 opposite corners and borders of Ω. At instant $i = 600$, most cells C_{pq} begin to lose some exposed individuals due to the movement towards the infected compartment and the number $E^{C_{pq}}$ becomes less and less important at further instants while $E^{C_{24}}$ does not exceed 2 exposed individuals.

In Fig. 7, when we suppose there are 40 susceptible people in cell C_{101}, and 50 others in each other cell, we can see that simultaneously, at instant $i = 150$, the number $I^{C_{110}}$ takes a value close/or equal to 12, while $I^{C_{pq}}$ in cells that are near to V_{110}, is less important, and as we move away from V_{110}, $I^{C_{pq}}$ is still zero. Similarly, at instant $i = 300$, the number $I^{C_{pq}}$ is zero at the 3 opposite corners and borders of Ω while it takes values between 1 and 3 in other cells, but $I^{C_{24}}$ is still very close to zero since very few people who have been infected there due to the effectiveness of the travel-blocking strategy. At instant $i = 450$, $I^{C_{pq}}$ takes values between 10 and 20 except at the opposite corners and borders, while C_{24} is still not containing more than 1 or 2 people in its infected compartment. Finally at last instants, $I^{C_{pq}}$ converge to 20, and to 22 in some cells at $i = 600$, except in C_{24} where $I^{C_{24}}$ does not exceed 1 or 2 infected individuals, and the number of infected individuals increases even in further cells and begin to decrease in cells which are close to V_{110} maybe due to mortality and also because not many individuals have been infected to move to the removed compartment, while $I^{C_{24}}$ does not exceed zero at $i = 900$.

In Fig. 8, when we suppose there are 40 susceptible people in cell C_{110}, and 50 others in each other cell, we can see that simultaneously, at instant $i = 150$, the number $R^{C_{110}}$ is still zero, while it increases to only 1 or 2 people at $i = 300$, and as we move away from V_{110}, $R^{C_{pq}}$ the number is still zero. Similarly, at instant $i = 450$, the number $R^{C_{pq}}$ is zero at the 3 opposite corners and borders of Ω while it takes values between 1 and 3 in other cells that are near to V_{110}, but we should note that $R^{C_{24}}$ is significantly negligible since very few people who have been infected there. Finally

at further instants, $R^{C_{pq}}$ converge to 3 at $i = 600$ in cells which are far away from the opposite corners and borders, except in C_{24} where $R^{C_{pq}}$ does not exceed 1 individual. $R^{C_{pq}}$ converge to 2.5 or 3 in most cells at $i = 900$, and the number of infected individuals is close to zero in C_{24} since not many individuals have been infected to move to the removed compartment.

5. Conclusion

In this paper, a multi-regions SEIRS discrete-time model was devised to describe epidemic dynamics when the source of infection comes from one region and which spreads to other regions via travel. A grid of cells where each cell represents a region, has been chosen for giving an example of simulations which could depict the spread of an epidemic in assembled regions in one domain. In fact, this kind of modeling approach has the advantage to exhibit the impact of the mobility on spreading an infection, even if the studied regions are not attached in reality. Based on the optimal control approach we suggested here, we have exhibit also, the impact of infection which comes from the vicinity of a cell. Finally, we have succeeded to show the effectiveness of the travel-blocking vicinity optimal control approach when it is applied to only one cell, an then, we proved that when we restrict movements of infected people coming from the vicinity of one region aiming to control, we can keep this region safe, or with insignificant infection.

Acknowledgement

This work is supported by the Systems Theory Network (Réseau Théorie des Systèmes), and Hassan II Academy of Sciences and Technologies-Morocco.

References

[1] M.A. Khan, A. Wahid, S. Islam, I. Khan, S. Shafie, T. Gul, Stability analysis of an SEIR epidemic model with non-linear saturated incidence and temporary immunity, Int. J. Adv. Appl. Math. andMech. 2(3)(2015) 1–14.
[2] A.A. Mohsen, H. Kasim, The effect of external source of disease on epidemic model, Int. J. Adv. Appl. Math. and Mech. 2(4) (2015) 53–63.
[3] S.C. Mpeshe, N. Nyerere, S. Sanga, Modeling approach to investigate the dynamics of Zika virus fever: A neglected disease in Africa, Int. J. Adv. Appl. Math. and Mech. 4(3) (2017) 14–21.
[4] O. Chaturvedi, S. Masupe, T. Masupe, SIRS Model For The Dynamics Of Non-Typhoidal Salmonella Epidemics, International Journal of Computational Engineering Research 3(10) (2013) 18–26.
[5] F. Paladini, I. Renna, L. Renna, A Discrete SIRS Model with Kicked Loss of Immunity and Infection Probability, In Journal of Physics: Conference Series 285(1) p. 012018. IOP Publishing, 2011.
[6] H. Zhao, J. Jiang, R. Xu, Y. Ye, SIRS Model of Passengers' Panic Propagation under Self-Organization Circumstance in the Subway Emergency, Mathematical Problems in Engineering 2014 (2014) .
[7] B.K. Mishra, S.K. Pandey, Dynamic model of worms with vertical transmission in computer network; Applied Mathematics and Computation 217(21) (2011) 8438–8446.
[8] O. Zakary, M. Rachik, I. Elmouki, On the analysis of a multi-regions discrete SIR epidemic model: an optimal control approach, International Journal of Dynamics and Control (2016) 1–14.
[9] O. Zakary, M. Rachik, I. Elmouki, A new analysis of infection dynamics: multi-regions discrete epidemic model with an extended optimal control approach, International Journal of Dynamics and Control (2016)1–10.
[10] O. Zakary, A. Larrache, M. Rachik, I. Elmouki, Effect of awareness programs and travel-blocking operations in the control of HIV/AIDS outbreaks: a multi-domains SIR model, Advances in Difference Equations, 2016(1) (2016) 1–17.
[11] O. Zakary, M. Rachik, I. Elmouki, A multi-regional epidemic model for controlling the spread of Ebola: awareness, treatment, and travel-blocking optimal control approaches, Mathematical Methods in the Applied Sciences (2016).
[12] J.M. Sánchez-Vizcaíno, L. Mur, B. Martínez-López, African swine fever: an epidemiological update, Transboundary and emerging diseases 59(s1) (2012) 27–35.
[13] M.D. Fray, D.J. Paton, S. Alenius, The effects of bovine viral diarrhoea virus on cattle reproduction in relation to disease control; Animal Reproduction Science 60 (2000) 615–627.
[14] F. Thiaucourt, A. Yaya, H. Wesonga, O.J.B. Huebschle, J.J. Tulasne, A. Provost, Contagious bovine pleuropneumonia: a reassessment of the efficacy of vaccines used in Africa, Annals of the New York Academy of Sciences 916(1) (2000) 71–80.
[15] M.J. Grubman, B. Baxt, Foot-and-mouth disease, Clinical microbiology reviews 17(2) (2004) 465–493.

[16] N. Afia, Manmohan Singh, David Lucy, Numerical study of SARS epidemic model with the inclusion of diffusion in the system; Applied Mathematics and Computation 229 (2014) 480–498.
[17] O. Zakary, M. Rachik, I. Elmouki, On the impact of awareness programs in HIV/AIDS prevention: an SIR model with optimal control, Int. J. Comput. Appl. 133(9) (2016) 1-6.
[18] G.P. Samanta, Permanence and extinction of a nonautonomous HIV/AIDS epidemic model with distributed time delay; Nonlinear Analysis: Real World Applications 12(2) (2011) 1163–1177.
[19] D. Chunxiao, N. Tao, Y. Zhu, A mathematical model of Zika virus and its optimal control, In Control Conference (CCC), 2016 35th Chinese, TCCT (2016) 2642–2645.
[20] D. Wandi, R. Hendon, B. Cathey, E. Lancaster, R. Germick, Discrete time optimal control applied to pest control problems; Involve, a Journal of Mathematics 7(4) (2014) 479-489.
[21] K. Dabbs, Optimal control in discrete pest control models, Thesis trace. tennessee. edu., 2010.
[22] S.P. Sethi, G.L. Thompson, What is optimal control theory? Springer, US, (2000) 1–22.